Received: 17 November 2021 | Revised: 17 March 2022 | Accepted: 22 April 2022

DOI: 10.1002/joc.7679

RESEARCH ARTICLE

International Journal of Climatology RMetS

The interannual synchronization of the heatwave days in Korea and western North Pacific tropical cyclone genesis frequency

Yumi Cha[1] | **Jae Won Choi**[2] | **Joong-Bae Ahn**[3]

[1]National Institute of Meteorological Sciences, Jeju, South Korea

[2]Institute for Basic Science, Pusan National University, Busan, South Korea

[3]Department of Atmospheric Sciences, Pusan National University, Busan, South Korea

Correspondence
Joong-Bae Ahn, Department of Atmospheric Sciences, Pusan National University, Geumjeong-gu, Busan 46241, South Korea.
Email: jbahn@pusan.ac.kr

Funding information
Korea Meteorological Administration, Grant/Award Number: KMA2018-00121

Abstract

This study conducted a correlation analysis between tropical cyclone genesis frequency (TCGF) in the western North Pacific (WNP) and heatwave days (HWD) in Korea during July and August for 1973–2018 and we found a strong positive correlation between them. This implied that the higher the TCGF in the WNP during July and August, the higher the HWD in Korea becomes. To examine the cause of the positive correlation between the TCGF during July and August in the WNP and the HWD in Korea, 15 years with the highest frequency and the lowest frequency out of the 46 years in the TCGF time series were selected and defined as high TCGF years and low TCGF years, respectively. According to the difference in atmospheric circulations between the two groups, in all layers of the troposphere, anomalous anticyclonic and cyclonic circulations were strengthened in the mid-latitude region of East Asia and in the WNP, respectively, which was similar to the Pacific-Japan (PJ) teleconnection pattern. The difference in the vertical meridional circulation averaged over the longitude range where Korea is located showed that anomalous upward and downward flows were strengthened in the WNP and in the latitude where Korea is located, respectively. This implied that the local Hadley circulation was strengthened during high TCGF years. Five hundred hectopascal wave activity flux originated from the North Atlantic, passed through the Scandinavian Peninsula, the North coast of Russia, and East Siberia before reaching Korea and the WNP. This spatial distribution was similar to the Scandinavia teleconnection pattern.

KEYWORDS

heatwave, Pacific-Japan (PJ) teleconnection pattern, Scandinavia teleconnection pattern, tropical cyclone genesis frequency

1 | INTRODUCTION

Heatwaves and tropical cyclones (TCs) are representative meteorological phenomena that have a great influence on South Korea. According to the Annual Disaster Report for two recent years, the number of deaths due to heatwaves was 48 in 2018 and 30 in 2019, which was 90.6 and 62.5%, respectively, of the total deaths caused by meteorological disasters, recording the most heat-related casualties in South Korea. According to Kim *et al.* (2014), the average number of deaths by heatwave was 21 per year, and the number has increased exponentially with

the increase in heatwave days (HWD) during the last two decades. The TC is the second most damaging natural disaster in South Korea (after the heatwave). Moreover, because TCs are accompanied by destructive wind and heavy rainfall, even one can cause enormous socioeconomic damage. In fact, TCs have long been the most devastating natural phenomenon in South Korea (Ministry of the Interior and Safety, 2017; 2018; 2019).

Higher global temperatures and sea surface temperatures (SSTs) increase the severe weather phenomena such as heatwaves and TCs, which are likely to become more frequent in the future (IPCC, 2019). Consequently, research related to these phenomena is being conducted in the Asian region, including South Korea, and there is concern that severe weather phenomena will increase in strength due to climate change. However, existing studies have mostly researched these two phenomena independently (heatwaves: Park *et al*., 2008; Kim *et al*., 2009; 2016; Suh *et al*., 2016; Yeh *et al*., 2018; Shin *et al*., 2018; TCs: Knutson *et al*., 2010; Choi *et al*., 2015; Moon *et al*., 2019). Matthews *et al*. (2019) pointed out the need for considering these two severe weather phenomena, which occur in warm seasons. They found that compound TC–heatwave events frequently occur, and the frequency is expected to increase in the future based on probabilistic simulations and climate change scenario experiments in the Northwest Pacific, the South Indian, and North Atlantic basins. They also project that highly destructive consequences will result from successive occurrences of TCs and heatwaves. Zhong *et al*. (2019) discovered through an analysis of TCs in the western North Pacific (WNP) and hot summer days in central eastern China that the more frequently TCs occur, the more hot days there are in central eastern China. They insisted that the reason was a feedback effect between hot summer days in central eastern China and TCs in the western North Pacific subtropical high (WNPSH), which dominates a large area from central eastern China to the Pacific Ocean near eastern Japan.

There have been few studies on the complex interactions between TCs and heatwaves in South Korea. However, correlations of these two phenomena have been estimated in previous studies (Lin, 2019). Although a TC is a mesoscale weather phenomenon, the development of a TC depends on the influence of the surrounding large-scale or synoptic-scale environment as it develops in the tropical western Pacific and moves northward. Because the TC moves along the edge of the WNPSH, expansion of the WNPSH is an important factor in addition to the factors affecting TCs in lower latitudes (e.g., monsoon gyre/trough, high SST, easterlies) (Cha *et al*., 2014). Furthermore, many studies argue that large-scale patterns in the higher latitudes, such as the Arctic Oscillation (AO), the North Atlantic Oscillation (NAO), and Pacific-Japan (PJ) teleconnection patterns, influence TC activities (Choi *et al*., 2010; Choi and Byun, 2010; Choi and Moon, 2012; Kim *et al*., 2012; Zhou and Cui, 2014).

Heatwaves have been proven in many studies to develop through interactions with synoptic-scale environments (Lee and Lee, 2016; Yoon *et al*., 2018; Lee *et al*., 2019; Yeo *et al*., 2019; Choi *et al*., 2020). Lee *et al*. (2020a) analysed extreme heatwaves in 2016 and 2018 and showed that the heatwave is related closely to the WNPSH, demonstrating that it begins as the WNPSH moves northward to the south sea of Korea, and South Korea enters the influence of the WNPSH. Yoon *et al*. (2018) and Lee *et al*. (2020b) classified types of synoptic weather patterns that cause heatwaves into three categories. When the edge of the WNPSH is located in Korea, heatwaves mainly occur, and the number of casualties is high. Although a heatwave is sometimes caused by an orographic influence, this is mainly limited to June, not the peak season of heatwave occurrences. Choi *et al*. (2020) and Lee *et al*. (2019) showed that teleconnection and global warming related to tropical convective activity contributed to heatwaves in 2016. Lee and Lee (2016) showed that the deep convection phenomenon of the South China Sea (SCS) provides conditions that cause heatwaves through the Rossby wave train, suggesting that tropical forcing is another major cause of heatwaves.

Unlike other seasons, even if TCs generally do not make landfall in Korea, most TCs that occur in July and August can indirectly affect the Korean Peninsula in various ways, such as extreme winds, storms, and heavy rains (KMA, 2011). Recently, it has been found that the TC occurrence/activity areas gradually move north (Kossin *et al*., 2014; Choi *et al*., 2015; Moon *et al*., 2015). This implies the increased possibility (within a relatively short period of time) of a TC directly or indirectly affecting the Korean Peninsula after its genesis. In addition, it is worth noting both heatwaves and TCs may have a correlation because the peak seasons are the same—July and August.

This study analysed the correlation between tropical cyclone genesis frequency (TCGF) in the WNP and heatwave days in Korea during July and August, and investigated the possible causes in large-scale environments and atmospheric circulations. That is, this study assumes that a correlation between the meteorological heatwave and the TC is possible because both hazardous phenomena occur in the summer and, in particular, TCs are not only affected by large- to synoptic-scale patterns in the WNP but they also influence the patterns, which may in turn affect heatwaves in the Korean Peninsula.

Section 2 introduces the data and analysis method. Section 3 presents the correlation between heatwaves in

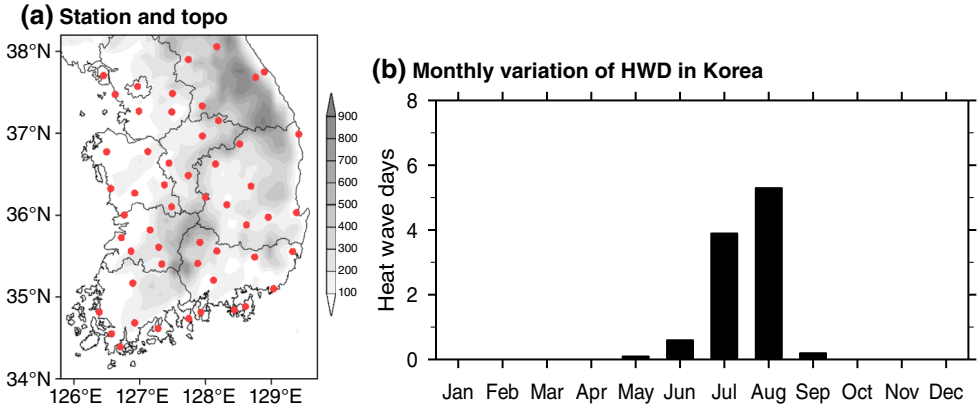

FIGURE 1 (a) Spatial distribution of data from observation stations, and (b) monthly heatwave day variations in Korea [Colour figure can be viewed at wileyonlinelibrary.com]

Korea and TC genesis in the WNP and the possible mechanisms causing them. Finally, section 4 summarizes these results.

2 | DATA AND METHODOLOGY

2.1 | Data

This study used data from the Regional Specialized Meteorological Center (RSMC) Tokyo – Typhoon Center to analyse TCs. In order to analyse large-scale environments and atmospheric circulation, the National Centers for Environmental Prediction/National Center for Atmospheric Research (NCEP/NCAR) Reanalysis dataset (Kalnay *et al*., 1996) was used. As for monthly global SST analysis, the National Oceanic and Atmospheric Administration (NOAA) Extended Reconstructed Sea Surface Temperature (ERSST) dataset (version 3) was used (Smith *et al*., 2008). NOAA's interpolated outgoing longwave radiation (OLR) was used to examine the state of convective activity (Liebmann and Smith, 1996). Precipitation data were from the Global Precipitation Climatology Project (GPCP) version 2.3 (Adler *et al*., 2003).

Furthermore, this study used surface air temperature (SAT), precipitation, and Palmer Drought Severity Index (PDSI) data recorded at 58 weather observation stations in Korea, which can be obtained from the Korea Meteorological Administration (KMA) at https://www.kma.go.kr. Spatial distributions of the 58 weather observation stations are shown in Figure 1a. Since the Ulleung-do and Jeju regions show unique weather characteristics of islands, the observation data in these two regions were excluded from this study. Since the number of weather observation stations in Korea has rapidly increased since 1973, this study used data after 1973. The data on HWD and tropical nights in Korea are officially provided on the KMA website at https://data.kma.go.kr/climate/. The KMA defines HWD as having a daily maximum temperature of 33°C or higher, and tropical nights have minimum temperatures of 25°C or higher. Since HWD mainly appear in July and August, as shown in Figure 1b, this study used July and August (J–A) mean data.

This study also used the East Asian summer monsoon index (EASMI) of Li and Zeng (2002, 2003, 2005), and the western North Pacific summer monsoon index (WNPSMI) provided on the website of the Asia-Pacific Data Research Center (APDRC) of the University of Hawaii (http://apdrc.soest.hawaii.edu/projects/monsoon/seasonal-monidx.html).

The Scandinavia teleconnection index was provided by the NOAA Climate Prediction Center at https://www.cpc.ncep.noaa.gov/data/teledoc/scand.shtml.

In addition, the Niño3 index provided by the NOAA Physical Sciences Laboratory (PSL) was used, available at https://psl.noaa.gov/gcos_wgsp/Timeseries/Nino3/.

2.2 | Methodology

The 2-tailed Student's *t* test was used to determine the significance of the results from this study (Wilks, 1995). The horizontal components of stationary Rossby wave propagation were calculated using the formula of Takaya and Nakamura (2001). The Pacific-Japan index is defined as the difference between two grid points (40°N, 150°E and 25°N, 125°E) for 850 hPa geopotential height anomalies (Wakabayashi and Kawamura, 2004; Kawamura and Ogasawara, 2006).

In this study, a TC is defined as one that occurs in the WNP and develops stronger than a tropical depression. Furthermore, the extratropical cyclone (EC) was also included in this study, because it causes significant human and property damage in the mid-latitude region of East Asia after a TC changes into an EC. The EC is transitioned from TC using the Regional Specialized Meteorological Centre (RSMC)-Tokyo Typhoon Center.

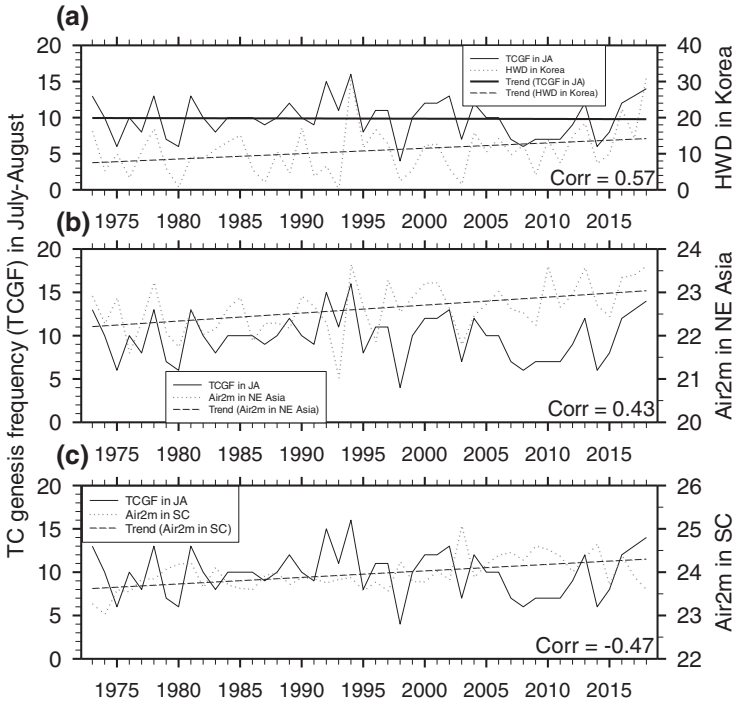

FIGURE 2 Time series of tropical cyclone genesis frequency (TCGF) in the western North Pacific (left): (a) heatwave days (HWD) in Korea (left upper panel), (b) Air2m in northeast Asia (left middle panel), and (c) Air2m in south China (left lower panel) in July–August (J–A)

3 | RESULTS

3.1 | Relationships between HWD in Korea and TCGF over the WNP

Figure 2a shows the TCGF in the WNP and the time series of HWD in Korea during July and August. Both time series show distinct interannual variations, rather than decadal variations. Meanwhile, the linear trend in the TCGF is statistically insignificant, because it shows little change, but HWD in Korea show an increasing linear trend due to the effect of global warming. This increasing linear trend is significant at the 95% confidence level. A close observation of these two time series reveals an in-phase trend between the two variables. Thus, a correlation analysis shows a strong positive correlation of 0.57. This is significant at the 99% confidence level, which means the higher the TCGF in the WNP during July and August, the more HWD in Korea. However, this correlation may change if the linear trend is removed from the two variables. Therefore, the correlation was analysed again after removing the linear trend, but it did not show a significant difference from the original result (Corr = 0.55, significant at the 99% confidence level). Furthermore, the correlation between tropical nights in Korea and TCGF in the WNP during July and August (not shown) was 0.60 (also significant at the 99% confidence level).

Meanwhile, to examine in more detail the correlation between HWD in Korea and TCGF in the WNP during July and August, the WNP was divided into the following four areas (Figure 3a): northwest (NW), southwest (SW), northeast (NE), and southeast (SE). This distinction was based on 16°N, 141°E according to the average TC genesis location for the 46 years under study. Among these four areas, the one that showed the highest correlation between TCGF and HWD in Korea during July and August is the SE with a correlation of 0.63. This is significant at the 99% confidence level. The next highest is the NW area, in which the TCGF during July and August and the HWD in Korea have a correlation of 0.52, also significant at the 99% confidence level. The correlation between the two variables in the other two regions is lower than 0.25, significant at the 90% confidence level. Consequently, the two variables tend to have a high correlation only in the NW and SE areas in the WNP. This appears to be because a monsoon trough develops from the northwest to the southeast direction in the tropical and subtropical WNP in general, and TCs tend to occur along this monsoon trough (Matsuura *et al*., 2003).

Therefore, the TCGF time series for July and August in the NW and SE areas were analysed (Figure 3b,c). The time series for TCGF in the NW area shows that the linear trend changed very little during the total 46-year analysis period (Figure 3b). However, when a correlation analysis was conducted after removing the linear trend from the two variables (because the linear trend of the HWD tended to increase in Korea), it was not much different from the original result (Corr = 0.51, significant at the 99% confidence level). The TCGF time series in the SE area has a strong interannual variation in general, but a weak interdecadal variation can be seen as well. The

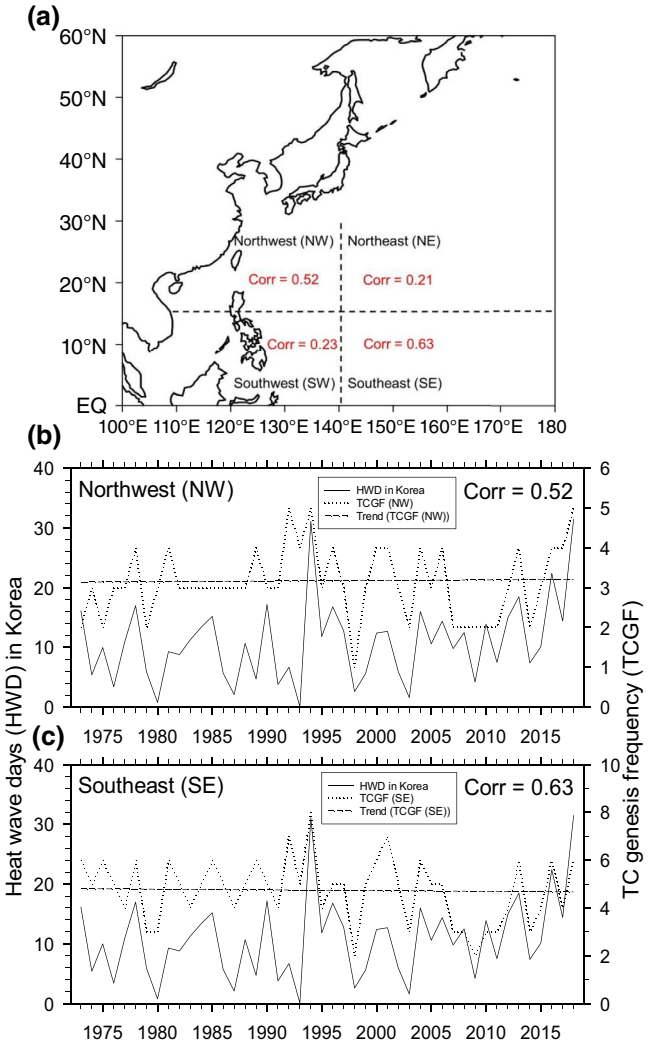

FIGURE 3 (a) Spatial distribution of correlation coefficients between HWD in Korea and TCGF in the northwest, southwest, northeast, and southeast areas over the western North Pacific in J–A. Time series of HWD in Korea versus (b) TCGF in the northwestern area, and (c) TCGF in the southeastern area over the western North Pacific in J–A [Colour figure can be viewed at wileyonlinelibrary.com]

time series also showed a rapidly increasing trend since the early 2010s (Figure 3c), but very little change in the linear trend, and the correlation did not change even when the linear trend was removed from the two time series (Corr = 0.62, significant at the 99% confidence level).

3.2 | Spatiotemporal distribution of air temperature and rainfall

To examine the reasons for a high positive correlation between the TCGF during July and August in the WNP and HWD in Korea, 15 years with the highest frequencies in the TCGF time series during July and August out of the 46 years under study and 15 years with the lowest frequencies in the 46 years were selected and defined as high TCGF years and low TCGF years, respectively (Table 1). Then, the mean difference between high TCGF years and low TCGF years was analysed. The mean HWD in Korea for all 46 years under study is 10.9 days; there are only 4 years among the high TCGF years that did not exceed the mean (1981, 1989, 1992, and 2002), and only 4 years among the low TCGF years did not exceed the mean (1983, 1995, 2008, and 2010). Hence, the mean HWD in high TCGF years is 15.4 days, but the mean HWD in low TCGF years is only 8.0 days, a difference of 7.4 days. This difference is significant at the 95% confidence level.

Here, we examine the spatial distribution of the mean SAT in July and August for the two groups (left panels of Figure 4a,b). The spatial distributions of the two groups appear similar in general. The northeast region in Korea shows the lowest SAT, whereas the southeast inland and

TABLE 1 Heat wave days (HWD) in Korea in high tropical cyclone genesis frequency (TCGF) years and low TCGF years

High TCGF years		Low TCGF years	
Year	**HWD**	**Year**	**HWD**
1973	16.2	1975	10.0
1978	17.0	1977	10.9
1981	9.3	1979	5.9
1989	4.7	1980	0.8
1992	6.7	1983	11.3
1994	31.1	1995	11.8
1997	12.8	1998	2.6
2000	12.4	2003	1.6
2001	12.7	2007	9.8
2002	5.9	2008	12.5
2004	16.0	2009	4.2
2013	18.5	2010	13.9
2016	22.4	2011	7.5
2017	14.4	2014	7.4
2018	31.5	2015	10.1
Average	15.4	Average	8.0

west inland areas show somewhat high SATs. However, most areas, excluding the northeast region in high TCGF years, show SATs higher than 30°C (left panel of Figure 4a), whereas in low TCGF years, most areas in Korea show SATs lower than 30°C (left panel of Figure 4b). The difference between the two groups shows a positive anomaly in all areas of Korea (left panel of Figure 4c), with the largest value in the central region of the east coast. Meteorologically, this region is known to have relatively high temperatures during the summer (Ko *et al*., 2006). The daily time series for the difference in SAT between the two groups indicates that high TCGF years have higher values from January to August, whereas low TCGF years have higher values from September to November (left panel of Figure 4d). The largest variations in SAT during the year appear in these two periods.

The reason SAT is high (low) may be because there are few (many) clouds in the atmosphere, and there is a low (high) possibility of precipitation. Hence, the spatial distribution of total rainfall in July and August for the two groups was analysed (right panels of Figure 4a,b). As expected, the spatial distributions of the two groups appear similar overall. Rainfall is relatively high in the northern region of Korea, whereas rainfall is low in the eastern and west coast regions. During high TCGF years, rainfall in the northern region of Korea is only 600 mm (right panel of Figure 4a), but during low TCGF years, it is higher than 700 mm in that region (right panel of Figure 4b). In particular, rainfall in the eastern region of Korea is lower during high TCGF years. The difference between the two groups shows a negative anomaly in most areas, excluding the northeast coastal region and part of the southeast coastal region (right panel of Figure 4c). This means there was more rainfall during low TCGF years than during high TCGF years. The largest difference appears in the northeast and southeast regions of Korea. The daily time series for the difference in rainfall between the two groups showed a strong negative anomaly during July and August, indicating that HWD could increase in Korea during high TCGF years (right panel of Figure 4d).

3.3 | Large-scale environments and atmospheric circulations

This study first analyses the difference in 2 m air temperature (Air2m) between the two groups of years in Asia (Figure 5). In the mid-latitude region of East Asia (30°–40°N), the Air2m was higher during high TCGF years, whereas the spatial distribution was higher during low TCGF years in other regions. Thus, we can see from this analysis that the increase in HWD during high TCGF years is likely to occur in the entire mid-latitude region of East Asia as well as in Korea. Then, East Asia was divided into NE Asia (30°–40°N, 115°–140°E) and South China (SC) (20°–30°N, 110°–120°E). The time series of area-averaged Air2m in each region and the TCGF time series during July and August in the WNP are shown in Figure 2b,c. First, the area-averaged Air2m time series in NE Asia shows strong interannual variations and weak interdecadal variations (Figure 2b). The linear trend in this time series is increasing, which is significant at the 95% confidence level. This increasing trend may be due to the effect of global warming. Furthermore, the two time series show an in-phase trend, and the correlation between these two variables showed a positive correlation of 0.43, which is significant at the 99% confidence level. This implies that if the TCGF in the WNP increases during July and August, there is a possibility that HWD in NE Asia can increase as well. Since the two time series show a distinctly increasing linear trend, the correlation may change if the linear trend is removed from the two time series. Therefore, the correlation was reanalysed after removing the trend. As a result, the correlation was higher than the original result (Corr = 0.46, significant at the 95% confidence level). The area-averaged Air2m time series in SC shows interannual and interdecadal variations (Figure 2c). This time series also shows an

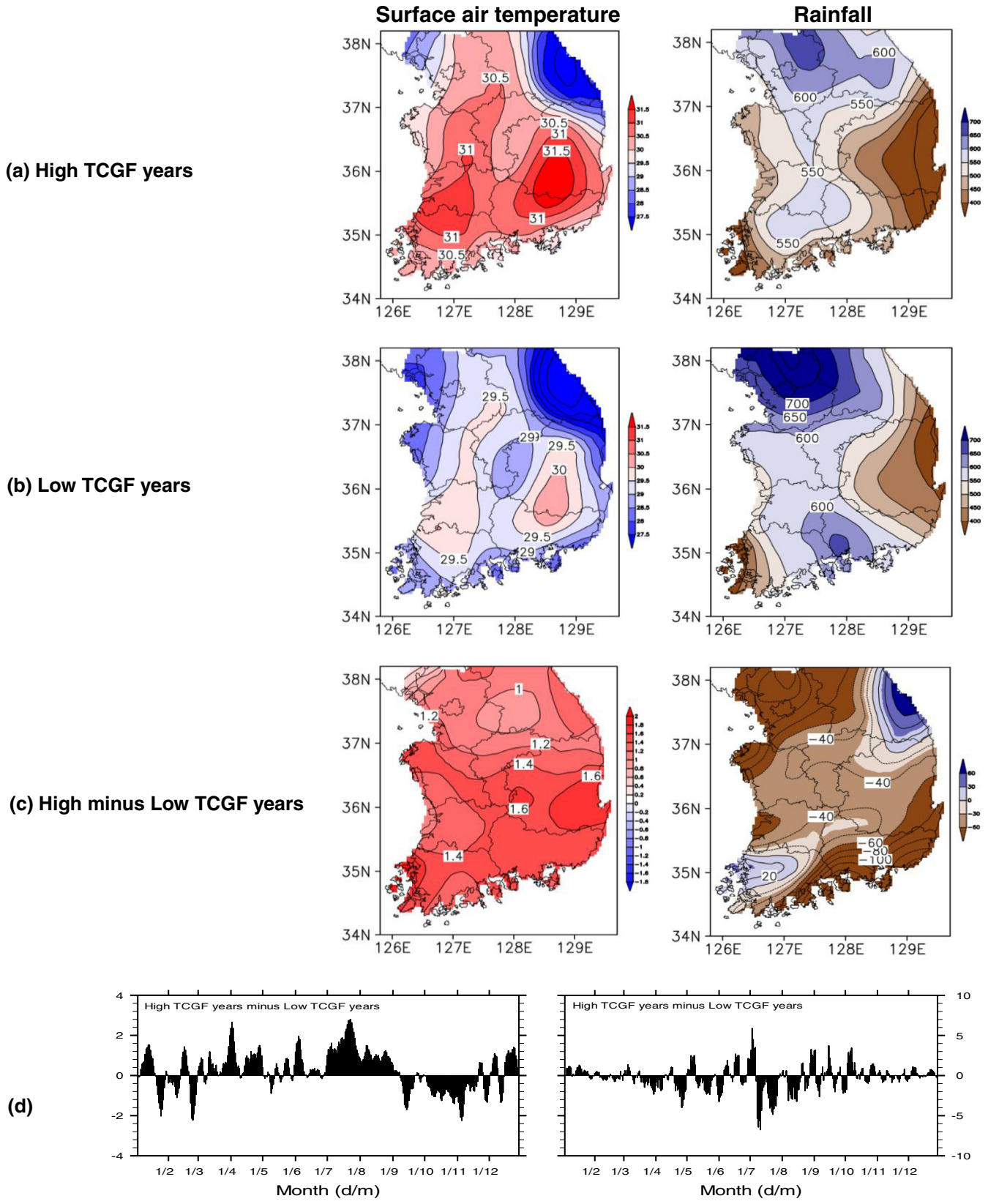

FIGURE 4 Spatial distributions of surface air temperature (left panel) and rainfall (right panel) in (a) high TCGF years, (b) low TCGF years, and (c) high-minus-low TCGF years in J–A. (d) Five-day running time series of mean surface air temperature (left panel) and rainfall (right panel) in high-minus-low TCGF years [Colour figure can be viewed at wileyonlinelibrary.com]

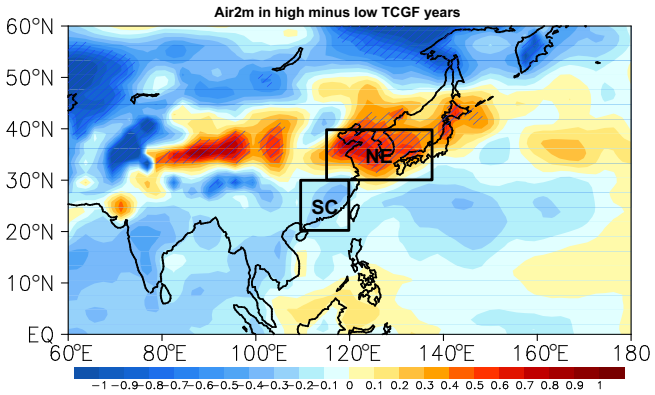

FIGURE 5 Composite differences in Air2m between high and low TCGF years in J–A. Hatched areas are significant at the 95% confidence level. The South China area is 20°–30°N, 110°–120°E, and the northeast (NE) Asia area is 30°–40°N, 115°–140°E [Colour figure can be viewed at wileyonlinelibrary.com]

increasing linear trend due to the effect of global warming, which is significant at the 95% confidence level. Furthermore, since these two time series show an out-of-phase trend, the correlation between the two variables was analysed. The result was −0.47, and this negative correlation is significant at the 99% confidence level. This indicates the possibility of a decreasing number of HWD in the SC area where the TCGF increases during July and August in the WNP. When the correlation was reanalysed after removing the linear trend from the two time series, the negative correlation was strengthened to some extent (to −0.49, which is significant at the 99% confidence level).

Meanwhile, the differences in air temperature between the two groups were analysed at a lower level (850 hPa), a middle level (500 hPa), and an upper level (300 hPa) (left panel of Figure 6). At 850 hPa, a warm anomaly was located in the mid-latitude region of East Asia, the centre of which includes Korea (left panel of Figure 6a). The warm anomaly in Korea was significant at the 95% confidence level. In addition, a weak warm anomaly appeared in the WNP in which TCs occur. Although weak, this warm anomaly must have influenced the increase in TCGF. At 500 hPa, a warm anomaly located in the mid-latitude region of East Asia shifted further north (left panel of Figure 6b). Thus, the southern region of Korea was under a cold anomaly, but this was not statistically significant. In the WNP, the area of the warm anomaly also shifted to the north. At 300 hPa, the warm anomaly in the mid-latitude region of East Asia moved much further north, and all of Korea experienced a cold anomaly (left panel of Figure 6c). That warm anomaly in the WNP strengthened a little more than at 850 and 500 hPa.

When both relative humidity and air temperature are high, people tend to feel more uncomfortable. Thus, the difference in relative humidity between the two groups was analysed (middle panel of Figure 6). At all levels, a negative anomaly was located over the Korean Peninsula. This is believed to be due to evaporation of water as subsidence strengthened from formation of an anomalous anticyclone in Korea. Meanwhile, in the WNP where TCs are generated, a positive anomaly appeared at every level. This is an important factor in increasing the TCGF. Gray (1975) pointed out that relative humidity at the lower level and the middle level is one of the important factors among the six physical parameters that influence TC genesis.

To examine the variations in spatial distributions of air temperature and relative humidity according to the levels analysed above, the differences in atmospheric circulations at those three levels were analysed (right panel of Figure 6). In all layers of the troposphere, anomalous anticyclonic circulations strengthened in the mid-latitude region of East Asia, and anomalous cyclonic circulations strengthened in the WNP. This was similar to the PJ teleconnection pattern (Nitta, 1986, 1987, 1989). The PJ pattern is an important pattern that influences the East Asian climate in summer (e.g., rainfall and air temperature) and TC genesis (Choi *et al.*, 2010). Therefore, the correlations of the PJ index with HWD in Korea and TCGF in the WNP during July and August were analysed (not shown). The results showed positive correlations of 0.43 and 0.41, respectively, significant at the 99% confidence level. This suggests that in Korea, subsidence developed, and water vapour evaporated, strengthening the anomalous anticyclone and resulting in negative relative humidity at every level. Moreover, as it moved from the lower level to the upper level, the anomalous anticyclone in the mid-latitude of East Asia shifted to the north. Consequently, as analysed above, the warm anomaly in the mid-latitude region of East Asia shifted to the north

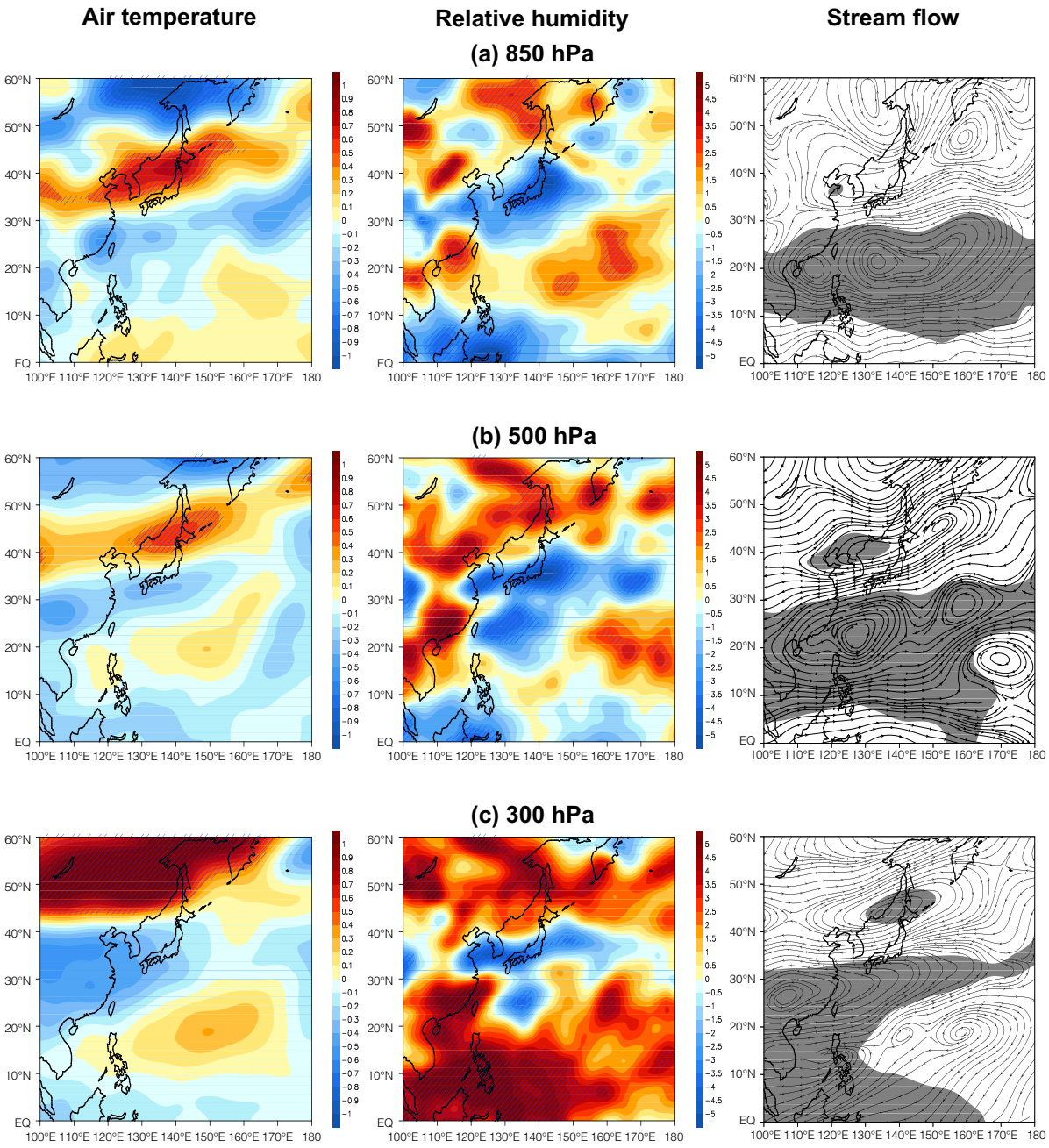

FIGURE 6 Composite differences in air temperature (left panel), percent relative humidity (middle panel), and stream flow (right panel) at (a) 850 hPa, (b) 500 hPa, and (c) 300 hPa between high and low TCGF years in J–A. Hatched areas in air temperature and relative humidity and the shaded area in stream flow are significant at the 95% confidence level [Colour figure can be viewed at wileyonlinelibrary.com]

toward the upper level. Meanwhile, the anomalous cyclone strengthening in the WNP at all three levels became an important background to the TCGF increase.

Increased or decreased numbers of HWD in Korea are associated with the locations of a western North Pacific subtropical high (WNPSH) and a Tibetan high (TH) (Wu *et al*., 2012). Hence, the degree of development in the WNPSH and the TH was analysed for the two groups of years (left panel of Figure 7). Here, the WNPSH (red line) and the TH (blue line) are defined as areas larger than 5,870 and 12,480 gpm, respectively. The WNPSH strengthened to the northwest over the western sea of Korea during high TCGF years (left panel of Figure 6a), whereas during low TCGF years, it expanded southwest into the southeastern region of China (left panel of Figure 6b). The TH was located a little to the north in high TCGF years, rather than in low TCGF years, and further expanded to the east during low TCGF

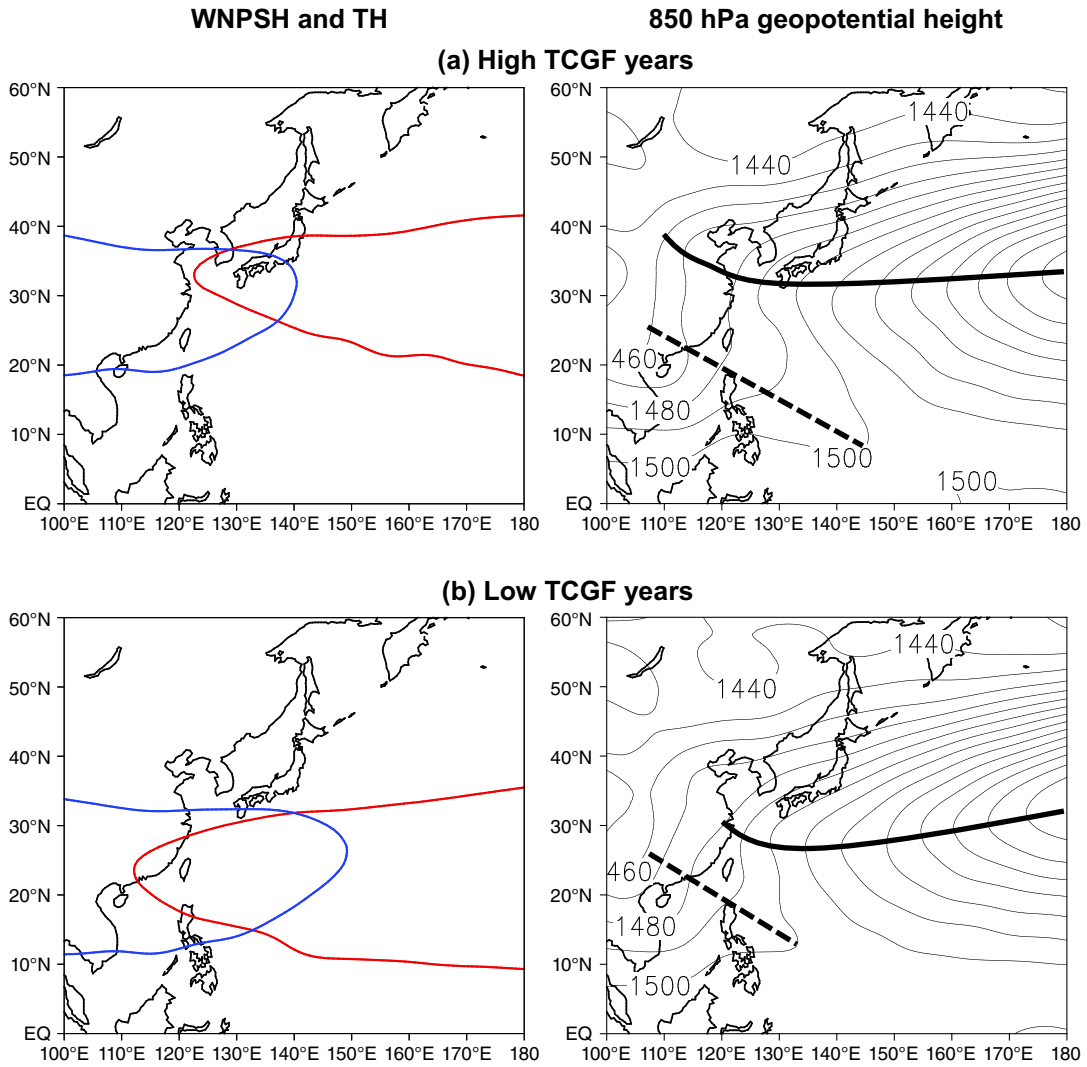

FIGURE 7 Spatial distributions of the western North Pacific subtropical high (5,870 gpm contour, red line in left panel) and the Tibetan high (12,480 gpm contour, blue line in left panel) in J–A, and composite maps of the 850 hPa geopotential height in (a) high TCGF years and (b) low TCGF years in J–A. In (b), dashed and solid lines denote the monsoon trough and the ridge of the WNPSH, respectively [Colour figure can be viewed at wileyonlinelibrary.com]

years. Hence, two high-pressure systems overlapped in Korea in high TCGF years. Thus, we can see that HWD increased as the solar radiation increased due to strengthening subsidence as the high-pressure systems were located in the upper and lower layers of the troposphere over Korea. Furthermore, during high TCGF years, the two high-pressure systems shifted to the north, and low-pressure systems strengthened in the WNP, thus increasing the TCGF.

To examine this, the 850 hPa geopotential height mean field was analysed for the two groups of years (right panel of Figure 7). Here, the dashed and solid lines indicate the monsoon trough and the ridge of the WNPSH, respectively. The ridge of the WNPSH expanded northwest to the northeastern region of China in high TCGF years (right panel of Figure 7a), but in low TCGF years, it expanded west to the eastern coast of central China (right panel of Figure 7b). As a result, in high TCGF years when the ridge of the WNPSH shifted more to the north, the monsoon trough strengthened, east to 145°E (right panel of Figure 7a). By contrast, in low TCGF years, the monsoon trough weakened, to only 130°E. This suggests that strengthening of the ridge of the WNPSH and the monsoon trough in high TCGF years is associated with the increase in HWD in Korea and the increase in TCGF in the WNP during July and August.

The anomalous anticyclone strengthened in the mid-latitude region of East Asia and the anomalous cyclone strengthened in the WNP can be associated with local Hadley circulation. To examine this, the difference in the vertical meridional circulation averaged over the longitude range of 120°–130°E where Korea is located was

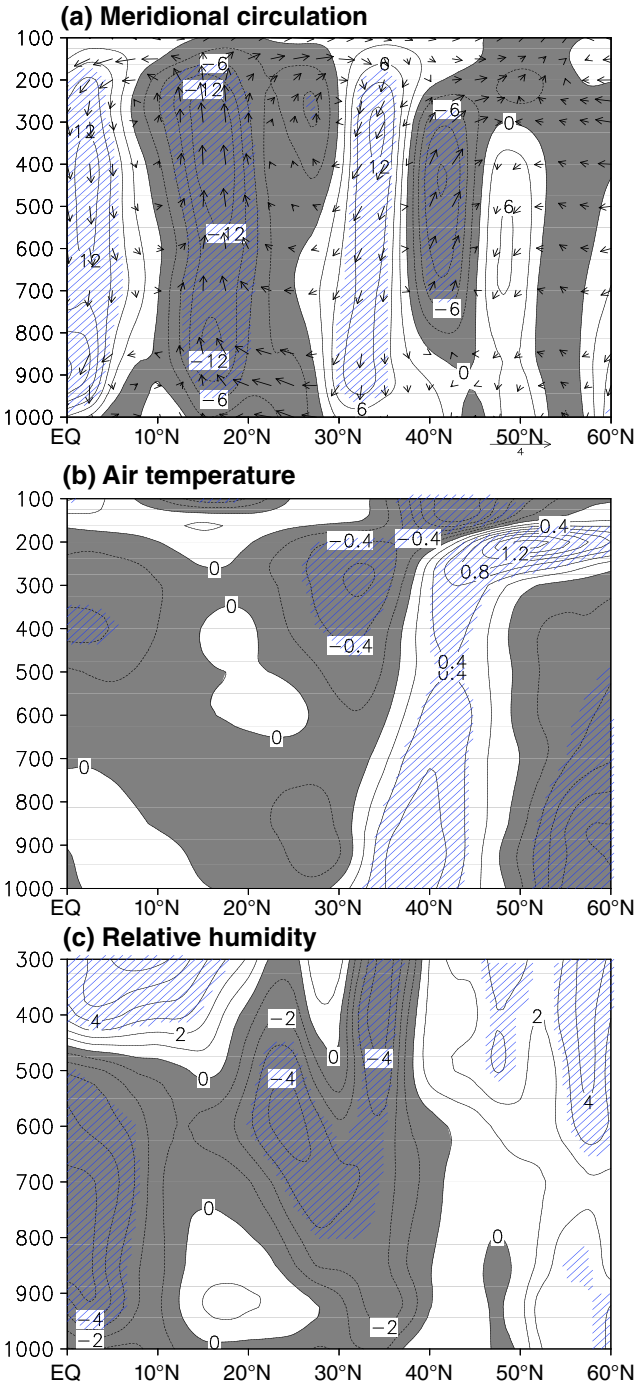

FIGURE 8 Composite differences in the latitude–pressure cross-sections of (a) vertical velocity (contours) and meridional circulations (vectors), (b) air temperature, and (c) relative humidity averaged along 120°–130°E between high and low TCGF years in J–A. The values of vertical velocity are multiplied by −100. Dashed areas are significant at the 95% confidence level, and shaded areas denote negative values. Contour intervals are 2^{-2} hPa·s^{-1}, 0.2°C, and 1% for vertical velocity, air temperature, and relative humidity, respectively [Colour figure can be viewed at wileyonlinelibrary.com]

analysed (Figure 8a). Anomalous upward flows strengthened at 10°–30°N where the WNP is located, and anomalous downward flows strengthened at 30°–40°N where Korea is located. In particular, the centre of anomalous upward motion in the WNP was located at 10°–20°N, and this is significant at the 95% confidence level. Furthermore, the centre of anomalous downward motion at 30°–40°N was distributed at 30°–35°N where South Korea is located, which is significant at the 95% confidence level. This anomalous vertical structure between the WNP and Korea means that the air rising in the WNP subsides in Korea. Therefore, the TCGF can

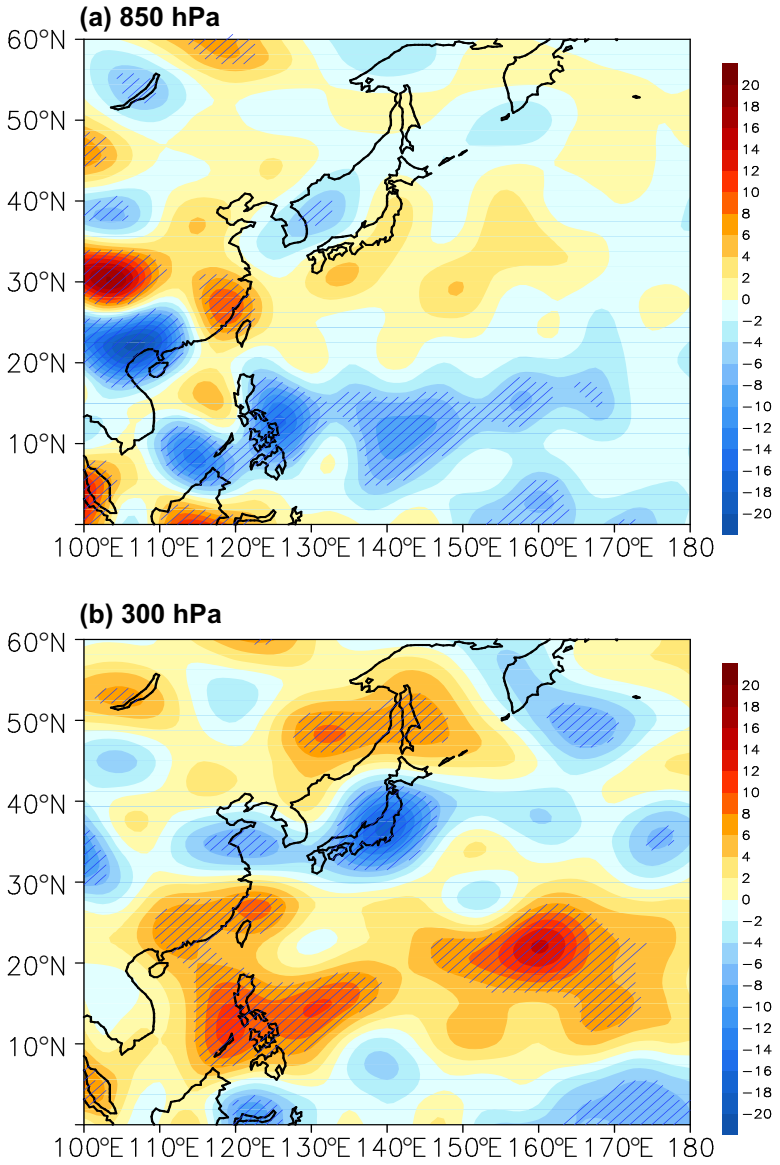

FIGURE 9 Composite differences in horizontal divergence (units: $s^{-1}*10^7$) between high and low TCGF years at (a) 850 hPa and (b) 300 hPa in J–A. Hatched areas are significant at the 95% confidence level [Colour figure can be viewed at wileyonlinelibrary.com]

increase in the WNP and can be an important background in which HWD can increase in Korea. As a result of this, in the vertical structure of air temperature, a warm anomaly appears in the lower level of 30°–40°E where Korea is located, and in the higher level, a cold anomaly appears (Figure 8b). This result is consistent with Figure 6, which shows that the warm anomaly in the mid-latitude region of East Asia shifted to the north toward the upper level. In the vertical structure of relative humidity, a negative anomaly appeared in every level of the latitude range for Korea (Figure 8c), and this characteristic is also consistent with Figure 6.

This local Hadley circulation that developed in high TCGF years can also be seen in the analysis of the differences in the horizontal divergence at lower and upper levels between the two groups of years (Figure 9). At 850 hPa, a negative anomaly appeared in the WNP and a positive anomaly appeared in the longitude range between 20°N and 30°N (Figure 9a). This means that anomalous convergence strengthened in the WNP, and anomalous divergence strengthened at 20°–30°N. However, Korea showed a weak negative anomaly. At 300 hPa, a positive anomaly strengthened in the WNP, and a negative anomaly was located in the longitude range between 30°N and 35°N where South Korea is located (Figure 9b). This implies that anomalous divergence strengthened in the WNP, and anomalous convergence strengthened in the mid-latitude region of East Asia. Thus, such a structure of horizontal divergence formed in the lower and upper levels implies that the air rising in the WNP falls in the mid-latitude region of East Asia, and this indicates the local Hadley circulation strengthened in high TCGF years.

In summer, the more HWD, the lower the precipitation, which can cause drought. Thus, the mean Palmer

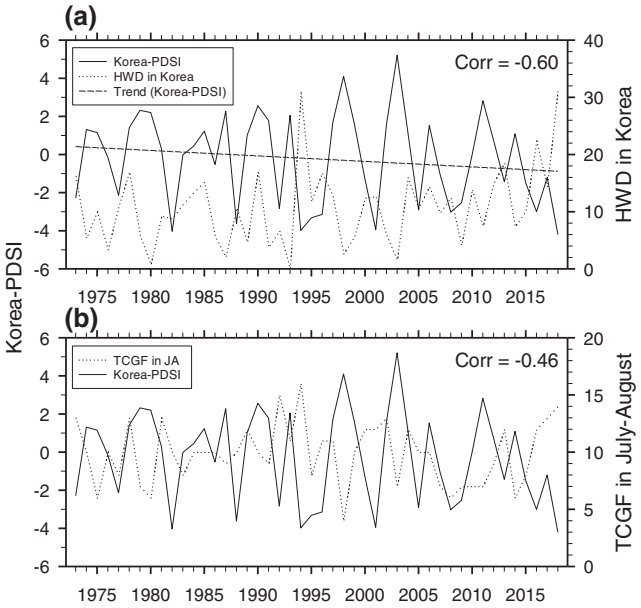

FIGURE 10 Time series of the Palmer Drought Severity Index in Korea from J–A for (a) HWD and (b) TCGF

Drought Severity Index in Korea during July and August and the time series of HWD in Korea were analysed (Figure 10a). A smaller PDSI implies a worse drought. The time series of the PDSI has strong interannual variations, and drought has worsened until recently due to the effect of climate change. This linear trend is significant at the 95% confidence level. Meanwhile, there is a distinct in-phase trend between the two variables. An analysis of the correlation between the two variables showed a correlation of −0.60. This high negative correlation is significant at the 99% confidence level. This means that in Korea, drought worsens as HWD increase. The two time series show a distinct change in the linear trend, but the correlation did not show a significant difference from the original correlation even when the linear trend was removed from the two time series (Corr = −0.58, significant at the 99% confidence level). In addition, the mean PDSI during July and August in Korea and the time series for TCGF in the WNP during July and August were analysed (Figure 10b). There is a distinct out-of-phase trend between the two variables. Analysis of the two variables showed a correlation of −0.46, significant at the 99% confidence level. This indicates that an increase in TCGF in the WNP strengthens drought in Korea, and this result is associated with the local Hadley circulation, as analysed above.

The anomalous anticyclone strengthening in the mid-latitude region of East Asia and the anomalous cyclone strengthening in the WNP can be associated with the EASM and the WNPSM, respectively. Hence, the time series of HWD in Korea and the mean EASMI and WNPSMI during July and August were analysed (Figure 11a,b). HWD in Korea and the EASMI showed opposite trends. When the correlation between the two variables was analysed, the result was −0.57 (Figure 11a). This negative correlation is significant at the 99% confidence level, implying that as the EASM strengthens (weakens), HWD in Korea become lower (higher). The linear trend in the EASMI showed little change. Consequently, the correlation did not show a significant difference from the original result when the linear trend was removed from the two time series (Corr = −0.56, significant at the 99% confidence level). Chen *et al.* (2019) indicated that, in active TC years, the EASM is stronger and the southerly winds in the lower troposphere advance farther north and reach higher latitudes. Meanwhile, the monsoon rain belt remains in the lower and middle reaches of the Yangtze River valley for a relatively short period, leading to less precipitation there. The time series of HWD in Korea and the mean WNPSMI during July and August were also analysed (Figure 11b). The two variables showed a distinct in-phase trend. When analysed, the correlation was positive at 0.56 (significant at the 99% confidence level). The WNPSMI has shown an increasing linear trend until recently, and this increasing linear trend is significant at the 90% confidence level. Therefore, the correlation was reanalysed after removing the linear trend from the two time series, and did not show a significant difference from the original result (Corr = 0.58, significant at the 99% confidence level). The above result suggests that an anomalous anticyclone strengthened in the mid-latitude region of East Asia during high TCGF years implies weakening of the EASM, and an anomalous cyclone strengthened in the WNP implies strengthening

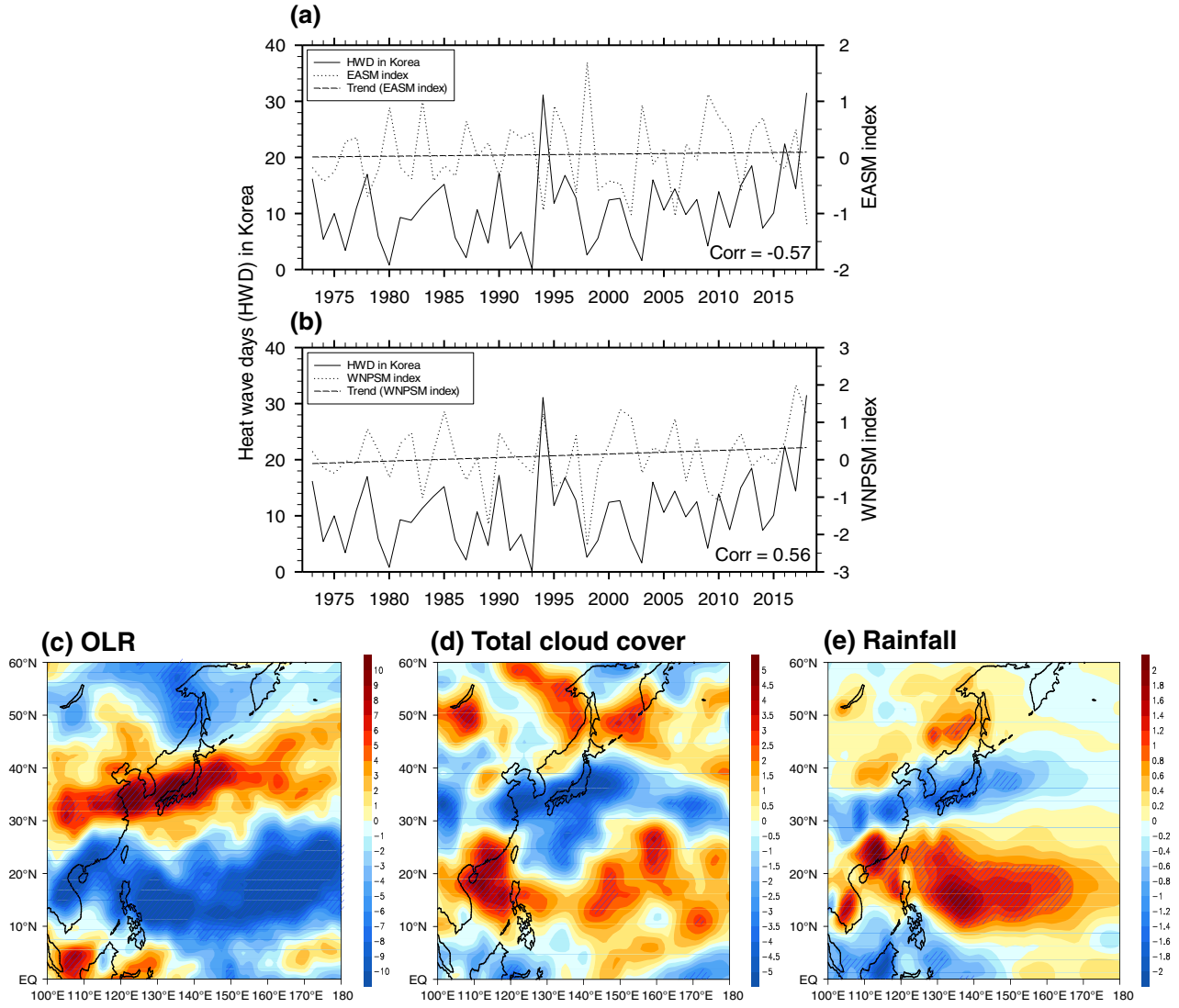

FIGURE 11 Time series of HWD in Korea versus (a) the East Asian summer monsoon (EASM) index and (b) the western North Pacific summer monsoon (WNPSM) index. Composite differences for (c) outgoing longwave radiation ($W \cdot m^{-2}$), (d) percentage of total cloud cover, and (e) rainfall between high and low TCGF years. In (c–e), hatched areas are significant at the 95% confidence level [Colour figure can be viewed at wileyonlinelibrary.com]

of the WNPSM. Regarding this, Choi *et al.* (2016) found that when the WNPSM strengthens, the TCGF increases, but the EASM tends to weaken.

To examine whether the EASM weakened in the mid-latitude region of East Asia during high TCGF years and whether the WNPSM strengthened in the WNP, the differences in the mean OLR, total cloud cover, and rainfall during July and August were analysed (Figure 11c–e). From the OLR analysis, a negative anomaly appeared in the WNP, whereas a positive anomaly appeared in the mid-latitude region of East Asia (Figure 11a). In particular, the centre of the positive anomaly in the mid-latitude region of East Asia was located in the zonal direction from central eastern China to Korea and Japan. The positive anomaly in this region is significant at the 95% confidence level. From the above result, we can see that convective activity strengthened in the WNP, whereas convective activity weakened in the mid-latitude region of East Asia. As a result, a large amount of total cloud cover was observed in the WNP, and a negative anomaly appeared in the mid-latitude region of East Asia (Figure 11d). The negative anomaly in Korea is significant at the 95% confidence level. The large amount of cloud formed by the strengthening of convective activity in the WNP led to a large amount of rainfall, and the opposite characteristic appeared in the mid-latitude region of East Asia (Figure 11e).

To examine whether the El Niño–Southern Oscillation (ENSO) influences HWD in Korea, the difference in mean SST during July and August between the two

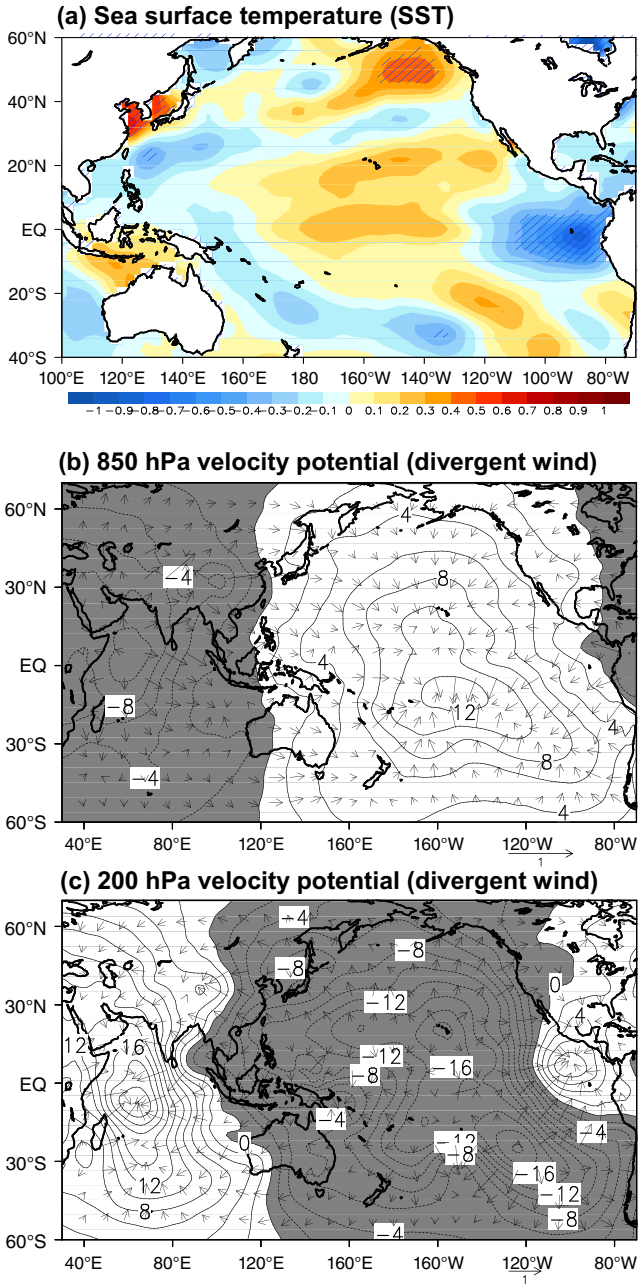

FIGURE 12 (a) Composite differences in SST between high and low TCGF years; hatched areas are significant at the 95% confidence level. Composite differences in (b) 850 hPa velocity potential and divergent wind and (c) 200 hPa velocity potential and divergent wind between high and low TCGF years. In (b, c), shaded areas denote negative anomalies, and the contour interval is 2 $m^2 \cdot s^{-1} 10^{-6}$ [Colour figure can be viewed at wileyonlinelibrary.com]

TABLE 2 Statistical result of partial correlation analysis

Control variable	Correlation variable	HWD	TCGF
Nino3 index	HWD	1.0	0.50
	TCGF	0.50	1.0

groups of years was analysed (Figure 12a). In general, a strong, cold anomaly appears in the equatorial eastern Pacific (EP), and this implies that the EP La Niña strengthens during high TCGF years. When the analysis results for the differences in velocity potential at lower and upper levels are examined, at the lower level, the centre of anomalous convergence was located in the east–west direction from the eastern sea of Australia to the offshore area of Peru. At the upper level, the centre of anomalous divergence was located in the subtropical and tropical central Pacific (Figure 12b,c). Therefore, the correlation between the Niño3.4 index and HWD in Korea

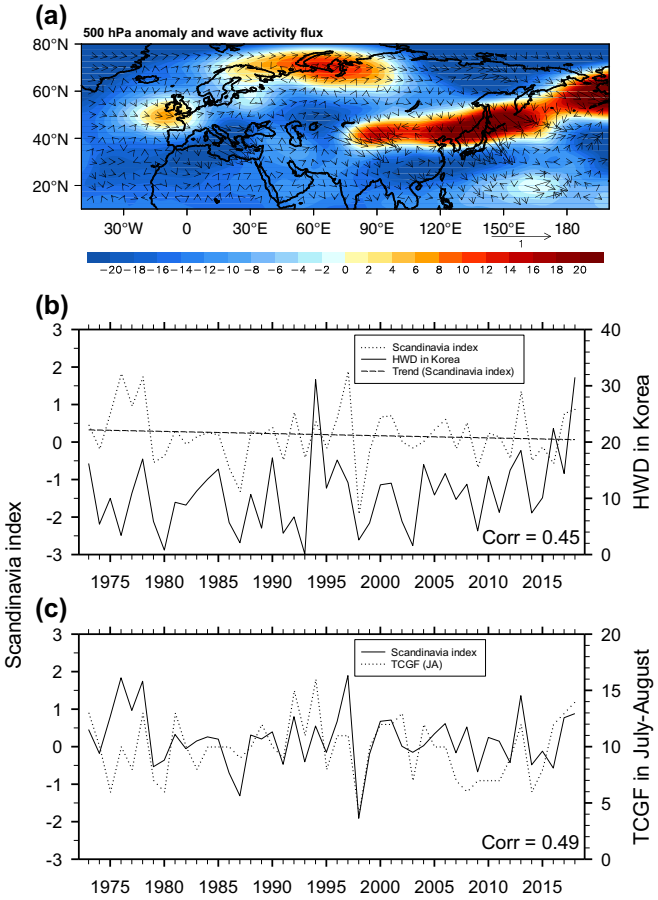

FIGURE 13 (a) Composite differences in 500 hPa geopotential height (shaded) and 500 hPa wave activity flux (vector). Time series of the Scandinavian Pattern Climate Index versus (b) HWD in Korea and (c) TCGF in J–A [Colour figure can be viewed at wileyonlinelibrary.com]

was analysed (not shown). These two variables showed a correlation of −0.27 at the 90% confidence level. However, the correlation analysis between the Niño3 index and TCGF in the WNP during July and August showed a correlation of −0.16, which is statistically insignificant. However, previous studies (Cao *et al.*, 2018; Liu and Chen, 2018; Zhao and Wang, 2018; Wu and Wang, 2019; Zhao *et al.*, 2019) have suggested that there are significant decadal changes in the correlation between WNP TCGF/monsoon and ENSO around 1990s (not significant before 1990s, but become significant after 1990s). Thus, a partial correlation analysis was conducted to examine whether the ENSO influenced the high positive correlation between HWD in Korea and TCGF in the WNP during July and August (Table 2). When the Niño3 index was set as a control variable, HWD in Korea and TCGF in the WNP during July and August showed a positive correlation of 0.50, significant at the 99% confidence level. This result suggests that the effect of ENSO on the high positive correlation between the two variables is small.

3.4 | Scandinavia teleconnection pattern

To determine what causes formation of the anomalous anticyclone in the mid-latitude region of East Asia and formation of the anomalous cyclone in the WNP during high TCGF years, 500 hPa wave activity flux was analysed (Figure 13a). The wave activity flux originates from the North Atlantic, then passes through the Scandinavian Peninsula and along the north coast of Russia and East Siberia before reaching Korea and the WNP. Also, wave activity flux moves toward north western region of China. Analysis of the difference in the 500 hPa geopotential height between the two groups of years showed a positive anomaly in the western sea of the U.K., the Scandinavian Peninsula, the northwestern coast of Russia, and the regions from Central Asia to the Bering Sea (shading in Figure 13a). This spatial distribution is similar to the Scandinavia pattern. Therefore, we can see that the anomalous anticyclone forming in the mid-latitude region of East Asia and the anomalous cyclone forming in the WNP during high TCGF years are

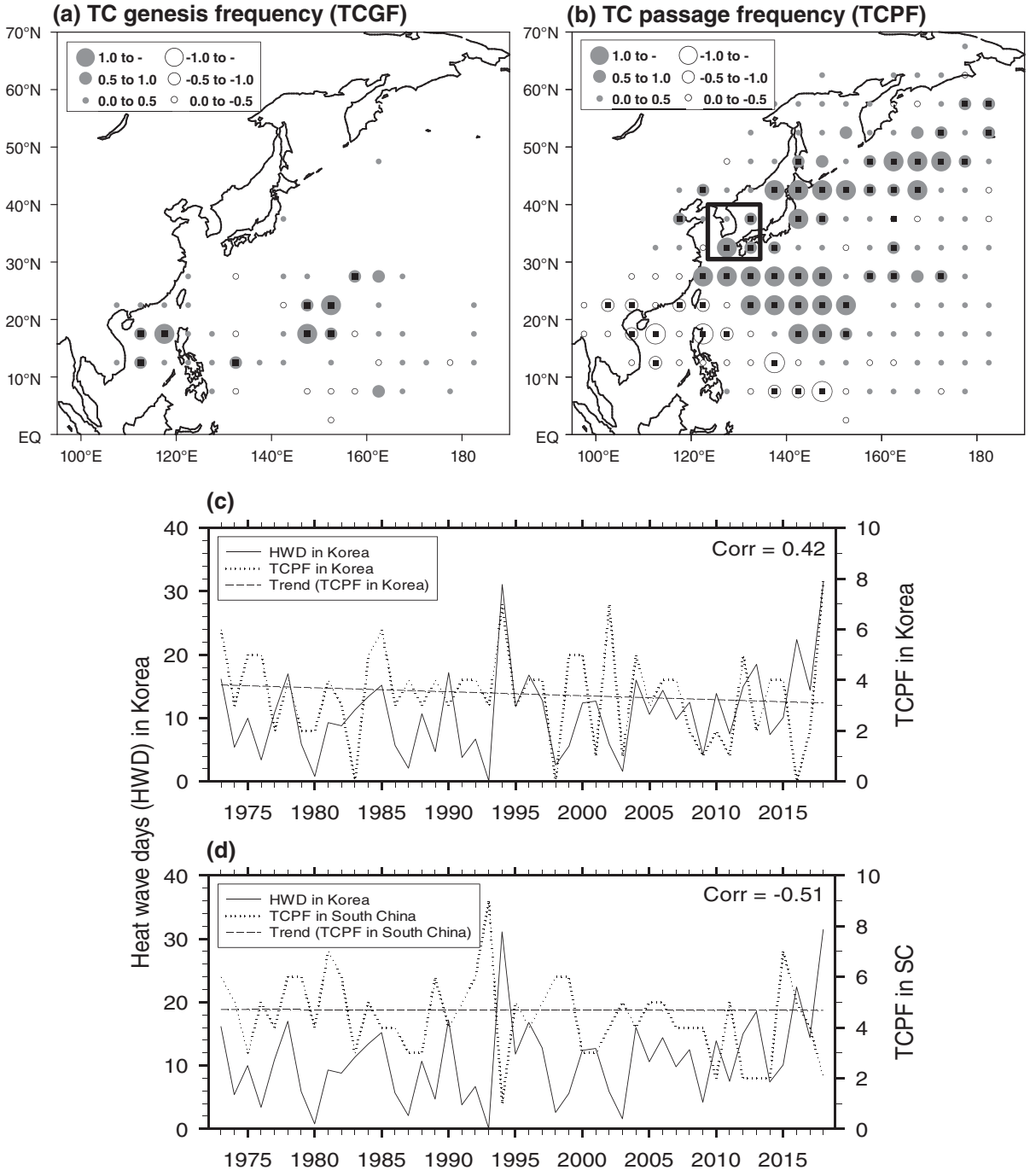

FIGURE 14 Differences in (a) TC genesis frequency and (b) TC passage frequency between high and low TCGF years. In (a, b), small squares inside the circles indicate that the differences are significant at the 95% confidence level. In (b), the square box denotes the Korea area (30°–40°N, 120°–130°E). Time series of HWD in Korea versus (c) TCPF in Korea and (d) TCPF in SC

associated with the Scandinavia teleconnection pattern. To examine whether HWD in Korea and TCGF during July and August are associated with the Scandinavia teleconnection pattern (SCAND), the Scandinavian Pattern Climate Index (SCANDI) and the time series between the two variables were analysed (Figure 13b,c). Both variables showed an in-phase trend with the SCANDI. The SCANDI showed a significant positive correlation of 0.45 with HWD in Korea at the 99% confidence level (Figure 13b). Correlation analysis with the TCGF in the WNP during July and August was positive: 0.49 at the 99% confidence level (Figure 13c). This shows that when the SCAND strengthens, HWD in Korea and TCGF in the WNP during July and August increase.

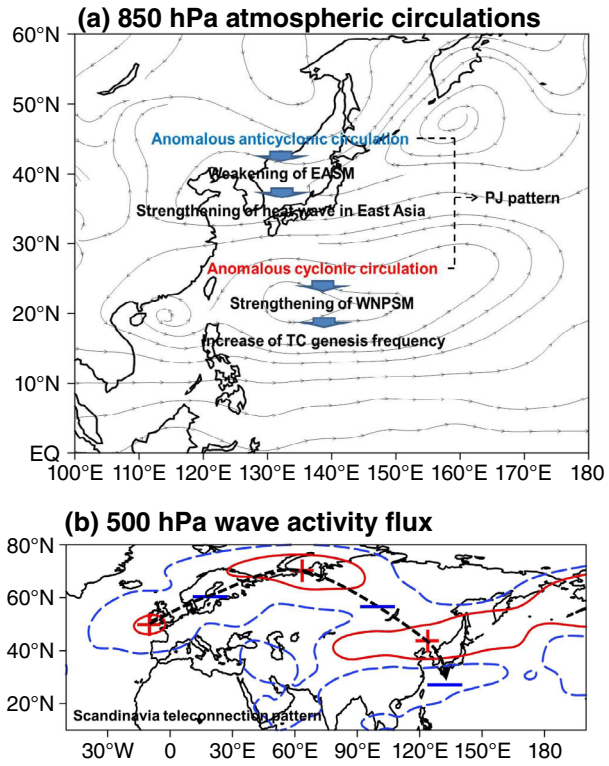

FIGURE 15 Schematic illustration of (a) 850 hPa anomalous atmospheric circulations and (b) 500 hPa wave activity flux occurring during the high TCGF years [Colour figure can be viewed at wileyonlinelibrary.com]

3.5 | TC activity

TCs can also influence HWD in Korea in summer. Therefore, the differences in TCGF and TC passage frequency (TCPF) during July and August between the two groups of years were analysed (Figure 14a,b). The spatial distribution of TCGF shows a higher genesis frequency during high TCGF years in general (Figure 14a). In particular, significantly large differences at the 95% confidence level appeared in the South China Sea and the northeastern sea of the WNP. The SCS and the northeast seas of the WNP show significantly large differences at the 95% confidence level. Meanwhile, spatial distribution of the TCPF (Figure 14b) showed a dipole pattern. In other words, a negative anomaly appeared in the Indochina Peninsula, the SCS, and the southeast region of China, and a positive anomaly appeared in the remaining areas. The cause of such a difference in spatial distribution of the TCGF between the two groups can be seen from analysis of the difference in the 500 hPa stream flow between the two groups (right panel of Figure 6b). In the Indochina Peninsula, the SCS, and the southeastern region of China, anomalous northerlies are strengthened by an anomalous cyclonic circulation forming in the WNP. These anomalous northerlies can play the role of steering flows that block TCs that move toward this area. By contrast, the mid-latitude region of East Asia (including Korea) is influenced by anomalous southeasterlies due to anomalous anticyclonic circulation, and these anomalous southeasterlies play the role of steering flows that move TCs to this region. This trend is associated with the location of the WNPSH for the two groups of years (left panel of Figure 7). TCs generally tend to move along the western edge of a WNPSH. Since the WNPSH is extended in the northwest to the western sea of Korea, TCs can easily move toward Korea and the mid-latitude region of East Asia. By contrast, during low TCGF years, the WNPSH extends southwest toward southeastern China, and TCs move to the Indochina Peninsula, the SCS, and the southeast region of China. Therefore, the time series of HWD in Korea and the TCPF in SC were analysed (Figure 14c,d). The TCPF in Korea shows an in-phase trend with HWD in Korea (Figure 14c), whereas it shows an out-of-phase trend with TCPF in the SC area (Figure 14d). In particular, the TCPF in Korea shows a decreasing linear trend, which is significant at the 90% confidence level. According to correlation analysis, HWD in Korea and the TCPF in Korea show a significant correlation of 0.42 at the 99% confidence level, whereas HWD in Korea and the TCPF in the SC area show a significant negative correlation of −0.51 at the 99% confidence level. Therefore, we can see that the TCPF in Korea increases,

but it decreases in the SC area during high TCGF years. Consequently, even if the TCPF in Korea increased during high TCGF years, it could not have contributed to mitigating heatwaves.

4 | SUMMARY AND CONCLUSIONS

This study analysed the correlations between TCGF in the WNP and HWD in Korea during July and August for the 46 years from 1973 to 2018. Analysis between these two variables showed a strong positive correlation. This implied that the higher the TCGF in the WNP during July and August, the more HWD in Korea.

To investigate causes of the high positive correlation between TCGF in the WNP during July and August and more HWD in Korea from the above analysis results, 15 high-frequency and low-frequency years in the 46-year TCGF time series were selected and defined as high TCGF and low TCGF years, respectively. An analysis of the difference in Air2m between the two groups of years showed that in the mid-latitude region, Air2m was higher during high TCGF years, whereas the spatial distribution was higher during low TCGF years in other regions. This analysis illustrates that the increase in HWD during high TCGF years is likely to occur in the entire mid-latitude region of East Asia as well as in South Korea.

The differences in the air temperature at the lower, middle, and upper levels of the troposphere between the two groups were analysed. At the lower level, a warm anomaly was located in the mid-latitude region of East Asia, at the centre of which Korea is located. Furthermore, the WNP, which is the area of TC genesis, showed a weak warm anomaly. At the middle level, a warm anomaly in the mid-latitude region of East Asia shifted more to the north, and the area of the warm anomaly in the WNP also shifted to the north. At the upper level, a warm anomaly in the mid-latitude region of East Asia moved much further north, and all of Korea was under a cold anomaly. In the WNP, the warm anomaly strengthened more at the lower and middle levels. In addition, the differences in relative humidity between the two groups of years were analysed. At all levels, a negative anomaly appeared over the Korean Peninsula. The reason for this was subsidence that strengthened from the formation of an anomalous anticyclone in Korea as well as increased evaporation. By contrast, a positive anomaly was found at every level in the WNP when a TC was generated.

According to the differences in atmospheric circulations between the two groups of years, at all levels of the troposphere, anomalous anticyclonic and cyclonic circulations strengthened in the mid-latitude region of East Asia and in the WNP, respectively. This is similar to the Pacific-Japan teleconnection pattern (Figure 15a). Chen *et al.* (2017) indicate that summertime frequent TC activities would create the poleward shift of the East Asian subtropical upper-level jet (EASJ) through a stimulated Pacific–Japan (PJ) teleconnection pattern as well as the changed large-scale meridional temperature gradient. On the contrary, in the inactive TC years, the EASJ is often located more southward than normal with an enhanced intensity. Therefore, TC activities over the WNP are closely related to the location and intensity of the EASJ in summer at the interannual time scale. Furthermore, anomalous anticyclone and cyclone strengthening in the mid-latitude region of East Asia and in the WNP was associated with weakening of the EASM and strengthening of the WNPSM, respectively.

The degrees of WNPSH and TH development were also analysed for the two groups. The WNPSH was strengthened northwest to the western sea of Korea during high TCGF years, whereas it extended southwest to the southeastern region of China during low TCGF years. The TH moved further north during high TCGF years, compared to low TCGF years. Instead, it extended further east during low TCGF years. Therefore, during high TCGF years, two high-pressure systems overlapped Korea. Thus, high-pressure systems were located at the lower and upper levels in Korea, and the strengthening of subsidence increased solar radiation, resulting in more HWD. Furthermore, during high TCGF years, the two high-pressure systems shifted north, strengthening the low-pressure system in the WNP, thus increasing TCGF.

The differences in mean SST during July and August between the two groups of years were analysed. In general, a cold anomaly appeared in the equatorial eastern Pacific, which implied strengthening of the EP La Niña during high TCGF years. Consequently, a partial correlation analysis was conducted to examine whether the ENSO influenced the high positive correlation between HWD in Korea and TCGF in the WNP during July and August. When the Niño3 index was set as a control variable, HWD in Korea and TCGF in the WNP during July and August showed a high positive correlation. This result suggested that the influence of ENSO on the high positive correlation between the two variables is not significant.

To determine the cause of the formation of anomalous anticyclones in the mid-latitude region of East Asia and the formation of anomalous cyclones in the WNP during the high TCGF years, 500 hPa wave activity flux was analysed (Figure 15b). The wave activity flux originated from the North Atlantic, passed through the Scandinavian Peninsula, and along the North coast of Russia

and East Siberia before reaching Korea and the WNP. The differences in the 500 hPa geopotential height between the two groups of years showed a positive anomaly in the western sea of the United Kingdom, the Scandinavian Peninsula, the northwestern sea of Russia, and the areas from Central Asia to the Bering Sea. This spatial distribution is similar to the Scandinavia teleconnection pattern. Therefore, we could see that anomalous anticyclones forming in the mid-latitude region of East Asia and anomalous cyclones forming in the WNP during high TCGF years are associated with the Scandinavia pattern.

The differences in TCPF during July and August between the two groups of years were also analysed. The Indochina Peninsula, the SCS, and the southeastern region of China showed a negative anomaly, whereas the other regions showed a positive anomaly. This suggests that TCPF could not contribute to mitigating heatwaves, even if TCPF increased in Korea at a time when TCGF is high.

AUTHOR CONTRIBUTIONS

Yumi Cha: Formal analysis. **Jae Won Choi:** Validation. **Joong-Bae Ahn:** Supervision.

ACKNOWLEDGEMENTS

This work was funded by the Korea Meteorological Administration Research and Development Program "Advancing Severe Weather Analysis and Forecast Technology" under Grant (KMA2018-00121).

ORCID

Joong-Bae Ahn https://orcid.org/0000-0001-6958-2801

REFERENCES

Adler, R.F., Huffman, G.J., Chang, A., Ferraro, R., Xie, P., Janowiak, J., Rudolf, B., Schneider, U., Curtis, S., Bolvin, D., Gruber, A., Susskind, J., Arkin, P. and Nelkin, E. (2003) The Version-2 Global Precipitation Climatology Project (GPCP) Monthly Precipitation Analysis (1979–present). *Journal of Hydrometeorology*, 4, 1147–1167.

Cao, X., Wu, R.G. and Xiao, X. (2018) A new perspective of intensified impact of El Niño–Southern Oscillation Modoki on tropical cyclogenesis over the western North Pacific around 1990s. *International Journal of Climatology*, 38, 4262–4275.

Cha, Y., Choi, K.S., Chang, K.H., Lee, J.Y. and Shin, D.S. (2014) Characteristics of the changes in tropical cyclones influencing the South Korean region over the recent 10 years (2001–2010). *Natural Hazards*, 74, 1729–1741.

Chen, X., Zhong, Z., Hu, Y., Zhong, S., Lu, W. and Jiang, J. (2019) Role of tropical cyclones over the western North Pacific in the East Asian summer monsoon system. *Earth and Planetary Physics*, 3(2), 147–156. https://doi.org/10.26464/epp2019018.

Chen, X., Zhong, Z. and Lu, W. (2017) Association of the poleward shift of East Asian subtropical upper-level jet with frequent tropical cyclone activities over the western North Pacific in summer. *Journal of Climate*, 30, 5597–5603. https://doi.org/10.1175/JCLI-D-16-0334.1.

Choi, J.W., Kim, B.J., Zhang, R.H., Park, K.J., Kim, J.Y., Cha, Y. and Nam, J.C. (2016) Possible relation of the western North Pacific monsoon to the tropical cyclone activity over the western North Pacific. *International Journal of Climatology*, 36, 3334–3345.

Choi, K.S. and Byun, H.R. (2010) Possible relationship between western North Pacific tropical cyclone activity and Arctic oscillation. *Theoretical and Applied Climatology*, 100, 261–274.

Choi, K.S. and Moon, I.J. (2012) Influence of the western Pacific teleconnection pattern on western North Pacific tropical cyclone activity. *Dynamics of Atmospheres and Oceans*, 57, 1–16.

Choi, K.S., Park, K.J., Kim, J.Y. and Kim, B.J. (2015) Synoptic analysis on the trend of northward movement of tropical cyclone with maximum intensity. *Journal of Environmental Sciences*, 36, 171–180 (in Korean).

Choi, K.S., Wu, C.C. and Cha, E.J. (2010) Change of tropical cyclone activity by Pacific-Japan teleconnection pattern in the western North Pacific. *Journal of Geophysical Research*, 115, D19114.

Choi, N., Lee, M.I. and Cha, D.H. (2020) Decadal changes in the interannual variability of heatwave in East Asia caused by atmospheric teleconnection changes. *Journal of Climate*, 33, 1505–1522.

Gray, W.M. (1975) *Tropical Cyclone Genesis*. Fort Collins, CO: Colorado State University. Department of Atmospheric Science Paper 234, 121 pp.

IPCC. (2019) Climate change and land: an IPCC special report on climate change, desertification, land degradation, sustainable land management, food security, and greenhouse gas fluxes in terrestrial ecosystems. In: Shukla, P.R., Skea, J., Buendia, E.C., Masson-Delmotte, V., Pörtner, H.-O., Roberts, D.C., Zhai, P., Slade, R., Connors, S., van Diemen, R., Ferrat, M., Haughey, E., Luz, S., Neogi, S., Pathak, M., Petzold, J., Pereira, J.P., Vyas, P., Huntley, E., Kissick, K., Belkacemi, M. and Malley, J. (Eds.) . Cambridge: Cambridge University Press, 874 pp. (in press).

Kalnay, E., Kanamitsu, M., Kistler, R., Collins, W., Deaven, D., Gandin, L., Iredell, M., Saha, S., White, G., Woollen, J., Zhu, Y., Leetmaa, A., Reynolds, R., Chelliah, M., Ebisuzaki, W., Higgins, W., Janowiak, J., Mo, K.C., Ropelewski, C., Wang, J., Jenne, R. and Joseph, D. (1996) The NCEP/NCAT 40-year reanalysis project. *Bulletin of the American Meteorological Society*, 77, 437–471.

Kawamura, R. and Ogasawara, T. (2006) On the role of typhoons in generating PJ teleconnection patterns over the western North Pacific in late summer. *SOLA*, 2, 37–40.

Kim, D.W., Jung, J.H. and Lee, J.S. (2014) Characteristics of heatwave mortality in Korea. *Atmosphere*, 24(2), 225–234 (in Korean).

Kim, J.A., Kim, K.R., Lee, C.C., Sheridan, S.C., Kalkstein, L.S. and Kim, B.J. (2016) Analysis of occurrence distribution and synoptic pattern of future heatwaves in Korea. *Journal of Climate Research*, 11(1), 15–27 (in Korean).

Kim, J.S., Cheuk, R., Li, Y. and Zhou, W. (2012) Effects of the Pacific-Japan teleconnection pattern on tropical cyclone activity and extreme precipitation events over the Korean Peninsula. *Journal of Geophysical Research*, 117, D18109.

Kim, J.Y., Lee, D.G. and Kysely, J. (2009) Characteristics of heat acclimatization for major Korean cities. *Atmosphere*, 19(4), 309–318 (in Korean).

Knutson, T.R., McBride, J.L., Chan, C.L.J., Emanuel, K., Holland, G., Landsea, C., Held, I., Kossin, J.P., Srivastava, A.K. and Sugi, M. (2010) Tropical cyclones and climate change. *Nature Geoscience*, 3, 157–163.

Ko, J.W., Baek, H.J., Kwon, W.T. and Park, J.Y. (2006) The characteristics of spatial distribution of temperature and regionalization in Korea. *Journal of Climate Research*, 1, 3–14.

Korea Meteorological Administration (KMA). (2011) *Typhoon White Book*. Seoul, South Korea: KMA, pp. 358.

Kossin, J.P., Emanuel, K.A. and Vecchi, G.A. (2014) The poleward migration of the location of tropical cyclone maximum intensity. *Nature*, 509, 349–352.

Lee, H.C., Cho, Y.J., Lim, B.H. and Kim, S.B. (2020b) Study on the association of casualties and classification of heatwave weather patterns in South Korea using *K*-means clustering analysis. *Journal of the Korean Society of Hazard Mitigation*, 20(3), 11–18 (in Korean).

Lee, H.D., Min, K.H., Bae, J.H. and Cha, D.H. (2020a) Characteristics and comparison of 2016 and 2018 heatwave in Korea. *Atmosphere*, 30(1), 1–15 (in Korean).

Lee, J.Y., Kim, H.J. and Jeong, Y.R. (2019) Influence of boreal summer intraseasonal oscillation on the 2016 heatwave over Korea. *Atmosphere*, 29(5), 627–637 (in Korean).

Lee, W.S. and Lee, M.I. (2016) Interannual variability of heatwaves in South Korea and their connection with large-scale atmospheric circulation patterns. *International Journal of Climatology*, 36, 4815–4830.

Li, J.P. and Zeng, Q.C. (2002) A unified monsoon index. *Geophysical Research Letters*, 29, 1274. https://doi.org/10.1029/2001GL013874.

Li, J.P. and Zeng, Q.C. (2003) A new monsoon index and the geographical distribution of the global monsoons. *Advances in Atmospheric Sciences*, 20, 299–302.

Li, J.P. and Zeng, Q.C. (2005) A new monsoon index, its interannual variability and relation with monsoon precipitation. *Climatic and Environmental Research*, 10, 351–365.

Liebmann, B. and Smith, C.A. (1996) Description of a complete (interpolated) outgoing longwave radiation dataset. *Bulletin of the American Meteorological Society*, 77, 1275–1277.

Lin, N. (2019) Tropical cyclones and heatwaves. *Nature Climate Change*, 9, 578–580.

Liu, Y. and Chen, G. (2018) Intensified influence of the ENSO Modoki on boreal summer tropical cyclone genesis over the western North Pacific since the early 1990s. *International Journal of Climatology*, 38, e1258–e1265.

Matsuura, T., Yumoto, M. and Iizuka, S. (2003) A mechanism of interdecadal variability of tropical cyclone activity over the western North Pacific. *Climate Dynamics*, 21, 105–117.

Matthews, T., Wilby, R.L. and Murphy, C. (2019) An emerging tropical cyclone–deadly heat compound hazard. *Nature Climate Change*, 9, 602-606. https://doi.org/10.1038/s41558-019-0525-6.

Ministry of the Interior and Safety (MOIS). (2017) Annual disaster report, p. 147.

Ministry of the Interior and Safety (MOIS). (2018) Annual disaster report, p. 217.

Ministry of the Interior and Safety (MOIS). (2019) Annual disaster report, p. 156.

Moon, I.J., Kim, S.H. and Chan, J.C.L. (2019) Climate change and tropical cyclone trend. *Nature*, 570, E3–E5.

Moon, I.J., Kim, S.H., Klotzbach, P. and Chan, J.C.L. (2015) Roles of interbasin frequency changes in the poleward shifts of the maximum intensity location of tropical cyclones. *Environmental Research Letters*, 10, 10400.

Nitta, T. (1986) Long-term variations of cloud amount in the western Pacific region. *Journal of the Meteorological Society of Japan*, 64, 373–390.

Nitta, T. (1987) Convective activities in the tropical western Pacific and their impact on the Northern Hemisphere summer circulation. *Journal of the Meteorological Society of Japan*, 65, 373–390.

Nitta, T. (1989) Global features of the Pacific-Japan oscillation. *Meteorology and Atmospheric Physics*, 41, 5–12. https://doi.org/10.1007/BF01032585.

Park, J.K., Jung, W.S. and Kim, E.B. (2008) Astudy on the influence of extreme heat on daily mortality. *Journal of Korean Society for Atmospheric Environment*, 24(5), 1511–1519 (in Korean).

Shin, J., Olson, R. and An, S.I. (2018) Projected heatwave characteristics over the Korean peninsula during the twenty-first century. *Asia-Pacific Journal of Atmospheric Sciences*, 54(1), 53–61.

Smith, T.M., Reynolds, R.W., Peterson, T.C. and Lawrimore, J. (2008) Improvements to NOAA's historical merged Land-Ocean surface temperature analysis (1880–2006). *Journal of Climate*, 21, 2283–2296.

Suh, M.S., Oh, S.G., Lee, Y.S., Ahn, J.B., Cha, D.H., Lee, D.K., Hong, S.Y., Min, S.K., Park, S.C. and Kang, H.S. (2016) Projections of high resolution climate changes for South Korea using multiple-regional climate models based on four RCP scenarios. Part 1: surface air temperature. *Asia-Pacific Journal of the Atmospheric Sciences*, 52(2), 151–169.

Takaya, K. and Nakamura, H. (2001) A formation of a phase-independent wave-activity flux for stationary and migratory quasigeosttrophic eddies on a zonally varying basic flow. *Journal of the Atmospheric Sciences*, 58, 608–627.

Wakabayashi, S. and Kawamura, R. (2004) Extraction of major teleconnection patterns possibly associated with the anomalous summer climate in Japan. *Journal of the Meteorological Society of Japan*, 82, 1577–1588.

Wilks, D.S. (1995) *Statistical methods in the atmospheric sciences*. New York, NY: Academic Press, 467 pp.

Wu, M. and Wang, L. (2019) Enhanced correlation between ENSO and western North Pacific monsoon during boreal summer around the 1990s. *Atmospheric and Oceanic Science Letters*, 12(5), 376–384.

Wu, Z., Jiang, Z., Li, J., Zhong, S. and Wang, L. (2012) Possible association of the western Tibetan Plateau snow cover with the decadal to interdecadal variations of northern China heatwave frequency. *Climate Dynamics*, 39, 2393–2402.

Yeh, S.W., Won, Y.J., Hong, J.S., Lee, K.J., Kwon, M., Seo, K.H. and Ham, Y.G. (2018) The record-breaking heatwave in 2016 over South Korea and its physical mechanism. *Monthly Weather Review*, 146, 1463–1474. https://doi.org/10.1175/MWR-D-17-0205.1.

Yeo, S.R., Yeh, S.W. and Lee, W.S. (2019) Two types of heatwave in Korea associated with atmospheric circulation pattern. *Journal of Geophysical Research: Atmospheres*, 124, 7498–7511.

Yoon, D.H., Cha, D.H., Lee, G., Park, C.Y., Lee, M.I. and Min, K.H. (2018) Impacts of synoptic and local factors on heat wave events over southeastern region of Korea in 2015. *Journal of Geophysical Research: Atmospheres*, 123(21), 12081–12096.

Zhao, H.K., Chen, S.H. and Klotzbach, P.J. (2019) Recent strengthening of the relationship between the western North Pacific monsoon and western North Pacific tropical cyclone activity during the boreal summer. *Journal of Climate*, 32, 8283–8299.

Zhao, H.K. and Wang, C.Z. (2018) On the relationship between ENSO and tropical cyclones in the western North Pacific during the boreal summer. *Climate Dynamics*, 52, 275–288.

Zhong, Z., Chen, X., Yang, X.Q., Ha, Y. and Sun, Y. (2019) The relationship of frequent tropical cyclone activities over the western North Pacific and hot summer days in central-eastern China. *Theoretical and Applied Climatology*, 138, 1395–1404.

Zhou, B.T. and Cui, X. (2014) Interdecadal change of the linkage between the North Atlantic Oscillation and the tropical cyclone frequency over the western North Pacific. *Science China Earth Sciences*, 57, 2148–2155.

How to cite this article: Cha, Y., Choi, J. W., & Ahn, J.-B. (2022). The interannual synchronization of the heatwave days in Korea and western North Pacific tropical cyclone genesis frequency. *International Journal of Climatology*, 1–22. https://doi.org/10.1002/joc.7679